Title
ELASTIC SCATTERING OF NEGATIVE PIONS ON PROTONS IN THE ENERGY RANGE 500 TO 1000 MeV

Authors
Helland, Jerome A.
Wood, Calvin D.
Devlin, Thomas J.
et al.

Publication Date
1963-11-18

UCRL-10495

University of California

Ernest O. Lawrence Radiation Laboratory

ELASTIC SCATTERING OF NEGATIVE PIONS ON
PROTONS IN THE ENERGY RANGE 500 TO 1000 MeV

Berkeley, California

DISCLAIMER

Submitted to Physical Review

UCRL-10495

UNIVERSITY OF CALIFORNIA

Lawrence Radiation Laboratory
Berkeley, California

AEC Contract No. W-7405-eng-48

ELASTIC SCATTERING OF NEGATIVE PIONS ON PROTONS IN THE ENERGY RANGE 500 TO 1000 MeV

Jerome A. Helland, Calvin D. Wood, Thomas J. Devlin, Donald E. Hagge, Michael J. Longo, Burton J. Moyer, and Victor Perez-Mendez

November 18, 1963

ELASTIC SCATTERING OF NEGATIVE PIONS ON PROTONS IN THE ENERGY RANGE 500 TO 1000 MeV*

Jerome A. Helland, Calvin D. Wood,† Thomas J. Devlin,‡
Donald E. Hagge, Michael J. Longo,§ Burton J. Moyer,
and Victor Perez-Mendez

Lawrence Radiation Laboratory
University of California
Berkeley, California

November 18, 1963

ABSTRACT

Differential cross sections for the elastic scattering of negative pi mesons on protons ($\pi^- p \rightarrow \pi^- p$) were measured at the Berkeley Bevatron at five laboratory kinetic energies of the pion between 500 and 1000 MeV. The results were least-squares fitted with a power series in the cosine of the center-of-mass scattering angle, and total elastic cross sections for $\pi^- p \rightarrow \pi^- p$ were obtained by integrating under the fitted curves. The coefficients of the cosine series are shown plotted vs the incident pion laboratory kinetic energy. These curves display as a striking feature a large value of the coefficient of $\cos^5 \theta^*$ peaking in the vicinity of the 900-MeV resonance. This implies that a superposition of $F_{5/2}$ and $D_{5/2}$ partial waves is prominent in the scattering at this energy, since the coefficients for terms above $\cos^5 \theta^*$ are negligible. One possible explanation is that the $F_{5/2}$ enhancement comes from an elastic resonance in the isotopic spin $T = 1/2$ state, consistent with Regge-pole formalism, and the $D_{5/2}$ partial-wave state may be enhanced by inelastic processes. At 600 MeV the values of the coefficients do not seem to demand the prominence of any single partial-wave state, although the results are compatible with an enhancement in the $J = 3/2$ amplitude. A table listing quantum numbers plausibly associated with the various peaks and "shoulders" seen in the $\pi^{\pm}$-p total-cross-section curves is presented.

I. INTRODUCTION

We report here the measurement of differential cross sections for the elastic scattering of negative pions on protons ($\pi^- p \rightarrow \pi^- p$), at incident pion lab kinetic energies of 533, 581, 698, 873, and 990 MeV. These measurements were made in conjunction with the experiment discussed in the preceding article[1] (hereafter referred to as I), and utilized the same equipment. The total-cross-section curves for both π^--p and π^+-p are shown in Fig. 1 of I.

The success of any theoretical attempt to treat related problems, such as nuclear forces and pion photoproduction, depends on an understanding of pion-nucleon scattering.[2] Although the 200-MeV peak has been clearly shown to be due to a single state in resonance,[3] the question of the origin of the 600- and 900-MeV peaks has not been definitely answered. The reason for making the measurements discussed in this article was to shed further light on the quantum numbers of the states associated with these higher peaks.

Early in the history of π^--p scattering studies, when the second and third maxima had not yet been resolved, Dyson[4] proposed a model to account for the broad "second maximum" at about 900 MeV. A single state in resonance would have to have J = 11/2, which he felt was unlikely, so he conceived of a π-π resonance with a relative momentum of 250 MeV/c, and in a T = 0 state so as to contribute nothing to π^+-p scattering. The large inelastic π-p scattering would be attributed to the incoming pion interacting with a cloud meson such that both escape from the nucleon.

Although the accumulation of experimental evidence, including the resolution of the broad peak into the two sharper maxima at 600 and 900 MeV, has not borne out all the predictions of Dyson's early model, the idea that a π-π interaction may be responsible for some of the high-energy phenomena still actively occupies the thinking of many theorists who are trying to explain the mechanisms of π-p scattering.

Since then other models have been proposed that employ various combinations of such concepts as the π-π interaction, pion-nucleon isobars, and the importance of inelastic processes.[5,6]

The quantum numbers predicted by such models are, of course, to be compared with the experimental data. The isotopic spin quantum number is readily fixed at $T = 1/2$, since these peaks do not appear in the π^+-p cross section, which is a pure $T = 3/2$ state. The π^--p system, however, is a mixture of $T = 1/2$ and $T = 3/2$ states.

The description of the (3/2, 3/2) resonance is quite complete, and was made in terms of phase shifts and partial waves.[7] At the energies of this experiment, however, we must include orbital angular-momentum states at least through F waves, which means that at least 28 parameters must be determined to give a complete phenomenological description of π-p scattering. Elastic-scattering measurements can determine constraints for these parameters, but other data, such as charge-exchange scattering and measurement of the polarization of the recoil proton, are needed before the solution to the problem can be regarded as uniquely determined in a mathematical sense.

A large number of elastic-scattering experiments have been done in the energy region of the higher peaks,[8,9] but most of them have a relatively low statistical accuracy. The results of this experiment are in essential agreement with those obtained by Wood et al.,[9] the main differences being that absolute normalizations, and hence total elastic cross sections, were obtained in the present experiment, and its instrumentation possessed a greater reliability through advances in techniques and devices since the time of the former experiment.

II. EXPERIMENTAL METHOD AND DATA ANALYSIS

The experimental arrangement for the measurement of the π^- differential cross sections is identical to that described in detail in I except for the following changes:

(a) The velocity spectrometer, used in I to discriminate between positive pions and protons of the same momentum, was turned off during these measurements.

(b) The currents of all the magnets in the pion beam were reversed for these measurements.

(c) The primary Bevatron ceramic target was moved slightly to compensate for trajectories of the opposite curvature (very slight) for the negative pions, because the target was located in a region not completely field-free.

The data of this experiment were analyzed by the same methods, and using the same computer program, as are described in I. The corrections were handled exactly like those applied there, only their magnitudes were slightly different.

Figure 1 shows the fraction of the total beam comprised of electrons, muons produced before B_2—the final bending magnet—and muons produced after B_2. The total muon and electron contamination varied from 8.2% of the total beam at 990 MeV, to 19.5% at 533 MeV.

III. EXPERIMENTAL RESULTS

The elastic differential cross sections are listed in Figs. 2 through 6, together with the errors (standard deviations), and the cosines of the scattering angles in the c. m. system. The values listed for $\cos\theta^* = 1.0$ were calculated by using dispersion relations.[10]

A least-squares fit[11] to the data was made with a curve having the equation

$$\frac{d\sigma(\theta^*)}{d\Omega^*} = \sum_{n=0}^{N} a_n \cos^n \theta^* , \qquad (1)$$

where N is the order of fit, and θ^* is the scattering angle in the c. m. system. The fitted curves, along with the corrected data points, are shown in Figs. 2 through 6. The dispersion-relations point was used to make the final fit at all energies. A fifth-order fit—i. e., N = 5—was used at 533 MeV, and a sixth-order fit was used at higher energies. The values of the coefficients a_n and their errors are listed in Table I, and are shown plotted in Fig. 7 with incident-pion lab kinetic energy as the abscissa. Figure 7 includes data from experiments other than this one.[8, 9]

The determinations of the correct orders of fit to be used and which of the data were to be rejected were made in the same manner as discussed in I.

Table II gives the value of χ^2 and $(\chi^2/d)^{1/2}$ for the chosen fit at each energy, where d is the number of degrees of freedom. Also listed in Table II are the total elastic cross sections for (π^--p → π^--p), as determined by integrating under the final fitted differential-cross-section curves. Figure 8 shows the following π^--p cross sections plotted vs incident-pion lab kinetic energy:

(a) Total π^--p cross section,[12]

(b) Total cross section for (π^--p → π^--p) (from Table II),

(c) Total charge-exchange cross section (π^--p → π^0-n) as determined from the data of Brisson et al.,[13]

(d) Total elastic cross section [sum of (b) and (c)],

(e) Total inelastic cross section [difference between (a) and (d)].

Some of these curves have relatively large errors.

Figure 9 shows the following cross sections for the pure T = 1/2 isotopic spin state:

(a) Total cross section, calculated by means of the relation

$$\sigma_{1/2} = 3/2\,\sigma^- - 1/2\,\sigma^+ \qquad (2)$$

where σ^- and σ^+ refer to the total cross sections for π^--p and π^+-p, respectively.

(b) Total elastic cross section, calculated by using Eq. (2), where, in this case, σ^- refers to total elastic cross section for π^--p, i. e., the sum of the charge-exchange cross section and the cross section for (π^--p $\rightarrow$ π^--p); σ^+ refers to the total elastic cross section for π^+-p.

(c) Total inelastic cross section; i. e., the difference between the above two.

The corresponding cross sections for the T = 3/2 isotopic spin state (π^+-p) are shown in I.

IV. DISCUSSION

The differential-cross-section curves (Figs. 2 through 6) exhibit two interesting features. First, the curve for 581 MeV is similar to that for 533 MeV, the main difference being the height of the forward peak ($\cos\theta^* = 1.0$). The increase in forward scattering in going from 533 to 581 MeV can possibly be attributed to an increase in the inelastic processes and is reflected in the elastic scattering as diffraction scattering. The shape of the inelastic-cross-section curve in Fig. 8. shows a behavior of this sort. This could imply that the 600-MeV peak in the total π^--p cross section is due to an enhancement in the inelastic processes, rather than the result of an elastic resonance. The second interesting feature is the shape of the 873-MeV curve (Fig. 5), i. e., the relatively pronounced hump at $\cos\theta^* = -0.8$.

In order to interpret the differential-cross-section curves it is useful to examine the plots of the coefficients of the powers of $\cos\theta^*$ as shown in Fig. 7. [In this connection it is recommended that the reader refer to the development of Eq. (16) in Sec. IV of I.] The most interesting aspect of Fig. 7 is the large positive value of a_5 which peaks near 900 MeV. The coefficient a_6 is nearly zero at this energy, implying that the scattering is negligible for those states having total angular momentum $J = 7/2$ or larger. The large value of a_5 must therefore come from a superposition of $F_{5/2}$ and $D_{5/2}$ partial waves. Furthermore, evidence can be adduced from some knowledge of the angular distribution in elastic charge exchange obtained by Chrétien et al.,[14] and also by Chiu et al. in a recent Berkeley experiment,[15] which requires the conclusion that both the $D_{5/2}$ and $F_{5/2}$ amplitudes belong to the $T = 1/2$ isotopic spin state.

One possible interpretation is that the $F_{5/2}$ amplitude enhancement is due to a resonant isobaric state of the nucleon, consistent with the $J = 5/2$ intersection of the nucleon Regge trajectory[16] having isotopic spin $T = 1/2$ and even parity. The $D_{5/2}$ enhancement may then be associated with the onset of absorptive channels with thresholds in this energy region (e. g., ρ-meson production and K-Λ production). It is difficult to limit such inelastic channels to the $T = 1/2$ state (although K-Λ satisfies this requirement), and the shoulder at 850 MeV in the $T = 3/2$ cross section may be a result of such processes.

At 600 MeV the values of the coefficients do not seem to indicate the prominence of any single partial-wave state. This is in agreement with the previously discussed interpretation of the 600-MeV peak; i. e., that it is the result of inelastic enhancements rather than an elastic resonance. However, it is noteworthy that the coefficient a_3, as shown in Fig. 7, demonstrates a marked departure at about 600 MeV from a general trend toward a negative maximum value that it attains near 900 MeV. This behavior suggests that the dominant character of a_3 may be to develop in the negative direction toward the 900-MeV resonance, but that the phenomenon at 600 MeV locally modifies this dominant behavior.

A locally prominent $D_{3/2}$ amplitude superimposed with the beginnings of the $F_{5/2}$ amplitude associated with the 900-MeV resonance could produce the behavior of a_3 in the region of 600 MeV. The fact that its local maximum is at an energy slightly greater than 600 MeV is appropriate to the increasing strength of the $F_{5/2}$ contribution as the energy is increased. Furthermore, a superposition of this $D_{3/2}$ amplitude with the $D_{5/2}$ amplitude, which we know also grows into strength near 900 MeV, is consistent with the variation of a_2 and a_4 with the opposite signs.

Deductions concerning the various amplitudes prominent in this energy region for the pion-nucleon interaction are also made from the photoproduction reactions. In particular, studies of polarization of the final-state proton in $\gamma p \rightarrow \pi^0 p$ by Maloy et al.,[17] and by Mencuccini et al.,[18] purport to show that if single-state enhancements are ascribed to the three "resonance" maxima observed in the $T = 1/2$ pion-nucleon interaction (corresponding respectively to laboratory pion scattering energies of 200, 600, and 900 MeV), then the second state is of parity opposite to the first and third. This would support a $P_{3/2}$, $D_{3/2}$, $F_{5/2}$ set of assignments. However, subsequent studies of $\gamma p \rightarrow \pi^+ n$ by Beneventano et al.,[19] show a prominent influence of a $D_{5/2}$ amplitude interfering with the $D_{3/2}$ (both in the $T = 1/2$ state), and they find no requirement for a "resonance," in the sense of a 90-deg real phase shift, in the region of the second cross section maximum. They suggest that the region of the second "resonance" is apparently more complicated than a single dominant-state phenomenon, and that interference with non-resonant amplitudes is appreciable. This situation, which is consistent with that here reported for pion-nucleon scattering, casts some uncertainty upon the initial interpretations of the polarization results in photoproduction.

The possible similarity of the 600-MeV peak in the T = 1/2 system and the 850-MeV shoulder in the T = 3/2 system has been alluded to by Carruthers[20] and others. The data of this and of the preceding article (I) allow some comparison. In both cases the rise in the elastic cross section is associated with an increase in the inelastic cross section from threshold up to a plateau value. The maximum in the elastic cross section is attained essentially at the "knee" of the inelastic variation; thereafter, the cross sections should be expected to fall off with increasing energy, because of the $1/p^2$ dependence, if for no other reason. In the T = 3/2 case the elastic cross section does not subside as the energy is increased, because of the immediate onset of the broad 1350-MeV resonance, and the result is the shoulder at about 850 MeV. Thus there is a gross similarity of these two phenomena, in the sense that they both are associated with rapidly rising inelastic effects.

If such effects are ascribed to an interaction of the incident pion with the pion cloud of the proton, it is possible to understand the fact that the threshold energies are not the same, since the π-π interaction states for π^--p are T = 0, T = 1, and T = 2, whereas for π^+-p they are T = 1 and T = 2. The effect of a T = 0 state of two pions is thus possible in the π^--p case, whereas such a combination could not be effective in π^+-p until energies are reached at which another pion could be produced. It has indeed been observed that the T = 0, π-π state is predominant in low-energy pion-pion interactions.[21] We may also include the possibility of an influence of virtual η_0 production upon the cross section even though production of free η_0's is known to be small at 600 MeV.[22] Such mechanisms need not enhance a particular state of the π-p system in a resonant sense in order to produce a maximum in the cross section.

In Table III we have listed quantum numbers that can speculatively be associated with the various known π-p phenomena. The conjectured total angular momenta are stated in parentheses; the values given are those possibly inferred from simple Regge-pole-trajectory behavior. The two peaks discovered by Diddens et al.,[23] at pion energies of 1950 MeV for π^--p, and 2370 MeV for π^+-p, are included in the table upon this basis of conjecture. The resonance points on a Regge plot are shown in Fig. 10, which illustrates the basis for the values given in parentheses in Table III. Diddens et al.[23] have discussed other assignments also to be considered for the two highest-energy resonances.

The authors would like to acknowledge the assistance by the same persons as in the preceding article.[1]

FOOTNOTES AND REFERENCES

* Work done under the auspices of the U. S. Atomic Energy Commission.

† Now at University of Utah, Salt Lake City, Utah.

‡ Now at Princeton University, Princeton, New Jersey.

§ Now at the University of Michigan, Ann Arbor, Michigan.

1. J. A. Helland, T. J. Devlin, D. E. Hagge, M. J. Longo, B. J. Moyer and C. D. Wood, Lawrence Radiation Laboratory Report UCRL-10378 Rev. 1, to be submitted to Phys. Rev. for simultaneous publication with this article.
2. Sergio Fubini, Rev. Mod. Phys. 33, 455 (1961).
3. (a) S. J. Lindenbaum and L. C. L. Yuan, Phys. Rev. 100, 306 (1955); (b) ibid. 111, 1380 (1958).
4. Freeman J. Dyson, Phys. Rev. 99, 1037 (1955).
5. Ronald F. Peierls, Phys. Rev. 118, 325 (1960).
6. J. S. Ball and W. R. Frazer, Phys. Rev. Letters 7, 204 (1961).
7. H. A. Bethe and F. de Hoffman, Mesons and Fields (Row, Peterson and Company, Evanston, Illinois, 1955), Vol.2: Mesons.
8. See references 26-40 of reference 9 (a).
9. (a) Calvin D. Wood (Ph. D. Thesis), Lawrence Radiation Laboratory Report UCRL-9507, October 1961 (unpublished).
   (b) C. D. Wood, T. J. Devlin, J. A. Helland, M. J. Longo, B. J. Moyer, and V. Perez-Mendez, Phys. Rev. Letters 6, 481 (1961).
10. See for example: J. W. Cronin, Phys. Rev. 118, 824 (1960).
11. P. Cziffra and M. J. Moravcsik, Lawrence Radiation Laboratory Report UCRL-8523 Rev., June 1959 (unpublished).
12. (a) H. C. Burrowes, D. O. Caldwell, D. H. Frisch, D. A. Hill, D. M. Ritson, R. A. Schluter, and M. A. Wahlig, Phys. Rev. Letters 2, 119 (1959).

(b) J. C. Brisson, J. F. Detoeuf, P. Falk-Vairant, L. van Rossum, and G. Valladas, Nuovo Cimento 19, 210 (1961).

(c) T. J. Devlin, B. J. Moyer, and V. Perez-Mendez, Phys. Rev. 125, 690 (1962).

13. J. C. Brisson, P. Falk-Vairant, J. P. Merlo, P. Sonderegger, R. Turlay, and G. Valladas, in Proceedings of the International Conference on Elementary Particles, Aix-en-Provence, 1961 (Centre d' Études Nucléaires, Saclay, France, 1961).

14. M. Chrétien (Brandeis Univ., Waltham, Mass.); F. Bullos et al. (Brown Univ., Providence); C. A. Bordner, Jr. et al. (Harvard Univ., Cambridge, Mass.); B. Nelson et al. (Massachusetts Inst. of Tech., Cambridge); and L. Guerriero and S. Waldner (Padua Università, Istituto di Fisica, and Istituto Nazionale di Fisica Nucleare, Padua); Neutral Meson Production in π^--p Collisions in the 1 BeV/c Region, TID-16677, May 1962 (unpublished).

15. Charles Chiu (Lawrence Radiation Laboratory, Berkeley, California), private communication.

16. G. F. Chew and S. C. Frautschi, Phys. Rev. Letters 8, 41 (1962).

17. J. O. Maloy, G. A. Salandin, A. Mandredini, V. Z. Peterson, J. I. Friedman and H. Kendall, Phys. Rev. 122, 1338 (1961).

18. C. Mencuccini, R. Querzoli, and G. Salvini, Phys. Rev. 126, 1181 (1962).

19. M. Beneventano, R. Finzi, L. Mezzetti, L. Paoluzi, and S. Tazzari, Nuovo Cimento 28, 1464 (1963).

20. P. Carruthers and H. A. Bethe, Phys. Rev. Letters 4, 536 (1960).

21. Howard J. Schnitzer, Phys. Rev. 125, 1059 (1962).

22. Janos Kirz (Ph. D. Thesis), Lawrence Radiation Laboratory Report UCRL-10720, March 1963 (unpublished).

23. A. N. Diddens, E. W. Jenkins, T. F. Kycia, and K. F. Riley, Phys. Rev. Letters 10, 262 (1963).

Table I. Coefficients of powers of cos θ^* (π^--p).

Coefficients	Pion kinetic energy in lab system (MeV)				
	533	581	698	873	990
a_0	0.431 ± 0.028	0.372 ± 0.043	0.243 ± 0.028	0.291 ± 0.046	0.293 ± 0.018
a_1	1.682 ± 0.120	2.188 ± 0.248	1.157 ± 0.102	-0.377 ± 0.152	-0.259 ± 0.063
a_2	2.240 ± 0.216	4.034 ± 0.523	4.431 ± 0.354	1.594 ± 0.591	-0.949 ± 0.247
a_3	-1.001 ± 0.591	-1.031 ± 1.121	-1.917 ± 0.463	-6.755 ± 0.786	-3.157 ± 0.343
a_4	0.554 ± 0.361	-1.887 ± 2.040	-5.201 ± 1.118	4.698 ± 1.878	8.118 ± 0.810
a_5	0.784 ± 0.594	1.223 ± 0.979	3.597 ± 0.464	15.551 ± 0.986	10.365 ± 0.431
a_6	---	1.745 ± 1.688	4.014 ± 0.881	2.473 ± 1.649	-0.162 ± 0.735

Table II. Values of χ^2, $(\chi^2/d)^{1/2}$, the number of data points,[a] the number of degrees of freedom, and the total elastic cross section with its error at each energy of the experiment.

Energy (MeV)	χ^2	$(\chi^2/d)^{1/2}$	Number of data points	Degrees of freedom	Elastic cross section
533	13.37	1.16	16	10	16.20 ± 0.50
581	19.02	1.38	17	10	19.95 ± 0.54
698	9.19	0.91	18	11	15.75 ± 0.28
873	20.26	1.30	19	12	26.58 ± 0.61
990	6.43	0.70	20	13	19.82 ± 0.24

[a] The dispersion-relations point, having been used in the curve fitting, is included in the number of data points.

Table III. Quantum numbers tentatively associated with π-p cross-section phenomena.

T = 1/2						T = 3/2				
Resonance ?	Isobaric energy (MeV)	Pion lab kinetic energy (MeV) ⊙	Parity	J	Orbital state	J	Parity	Pion lab kinetic energy (MeV)	Isobaric energy (MeV)	Resonance ?
yes	938	--	+	1/2	P	3/2	+	195	1236	yes
--	1510	600	-	3/2	D	(5/2)	-	850	1660	--
yes	1690	900	+	5/2	F	7/2	+	1350	1920	yes
--	--	--	--	--	G	--	--	--	--	--
(yes)	2190	1950	(+)	(9/2)	H	(11/2)	(+)	2370	2360	(yes)
--	--	--	--	--	I	--	--	--	--	--

FIGURE CAPTIONS

Fig. 1. Muon and electron contamination in pion beam plotted vs incident pion lab kinetic energy.

Fig. 2. The π^--p differential-cross-section curve for an incident pion lab kinetic energy of 533 MeV.

Fig. 3. The π^--p differential-cross-section curve for an incident pion lab kinetic energy of 581 MeV.

Fig. 4. The π^--p differential-cross-section curve for an incident pion lab kinetic energy of 698 MeV.

Fig. 5. The π^--p differential-cross-section curve for an incident pion lab kinetic energy of 873 MeV.

Fig. 6. The π^--p differential-cross-section curve for an incident pion lab kinetic energy of 990 MeV.

Fig. 7. Coefficients of power series in cos θ^* plotted vs the incident pion lab kinetic energy.

Fig. 8. The π^--p cross sections.

Fig. 9. The T = 1/2 π-p cross sections.

Fig. 10. Pion-nucleon Regge plots.

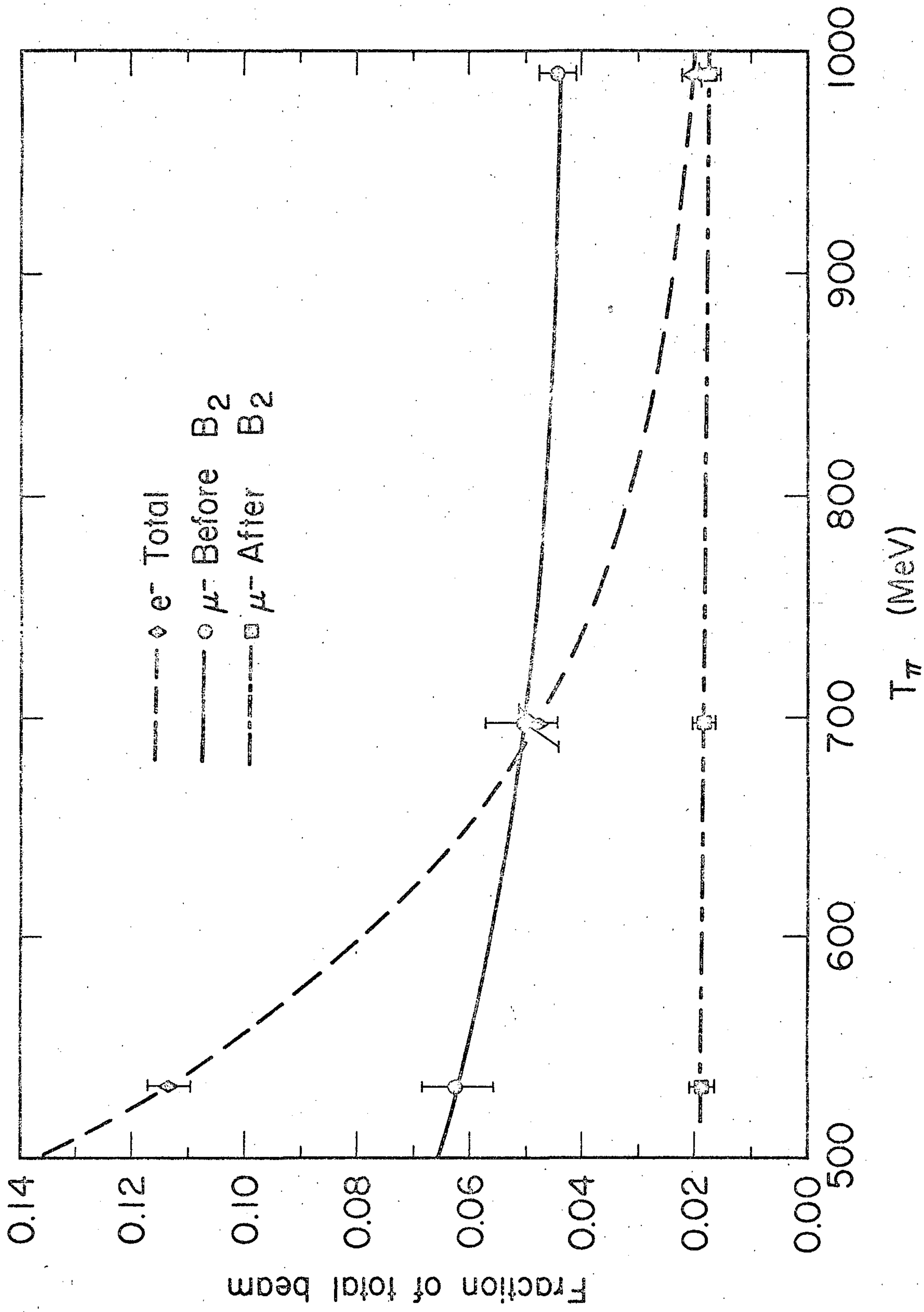

MU-32512

Fig. 1.

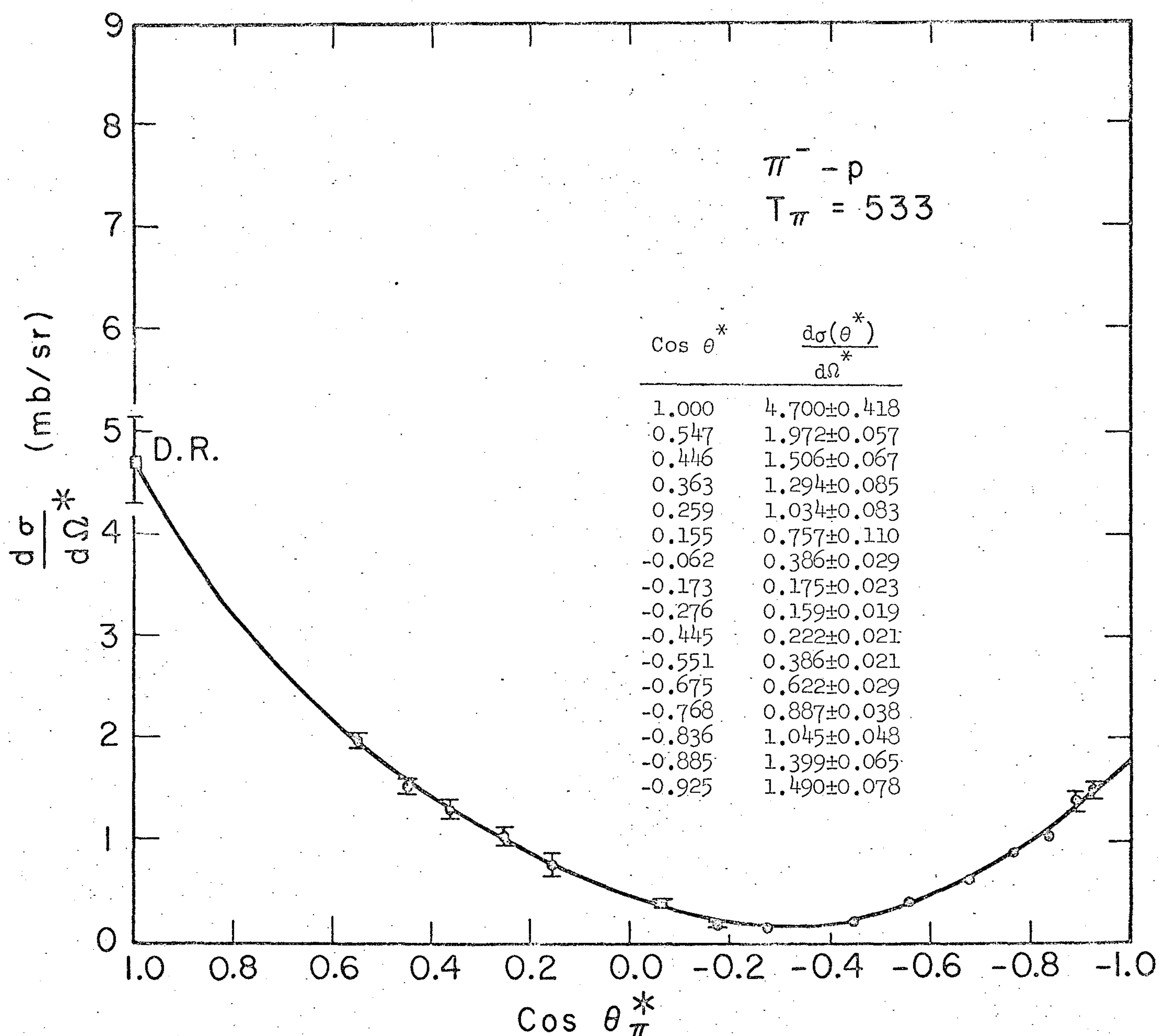

Cos θ^*	$\frac{d\sigma(\theta^*)}{d\Omega^*}$
1.000	4.700±0.418
0.547	1.972±0.057
0.446	1.506±0.067
0.363	1.294±0.085
0.259	1.034±0.083
0.155	0.757±0.110
-0.062	0.386±0.029
-0.173	0.175±0.023
-0.276	0.159±0.019
-0.445	0.222±0.021
-0.551	0.386±0.021
-0.675	0.622±0.029
-0.768	0.887±0.038
-0.836	1.045±0.048
-0.885	1.399±0.065
-0.925	1.490±0.078

Fig. 2.

MU-27308-A

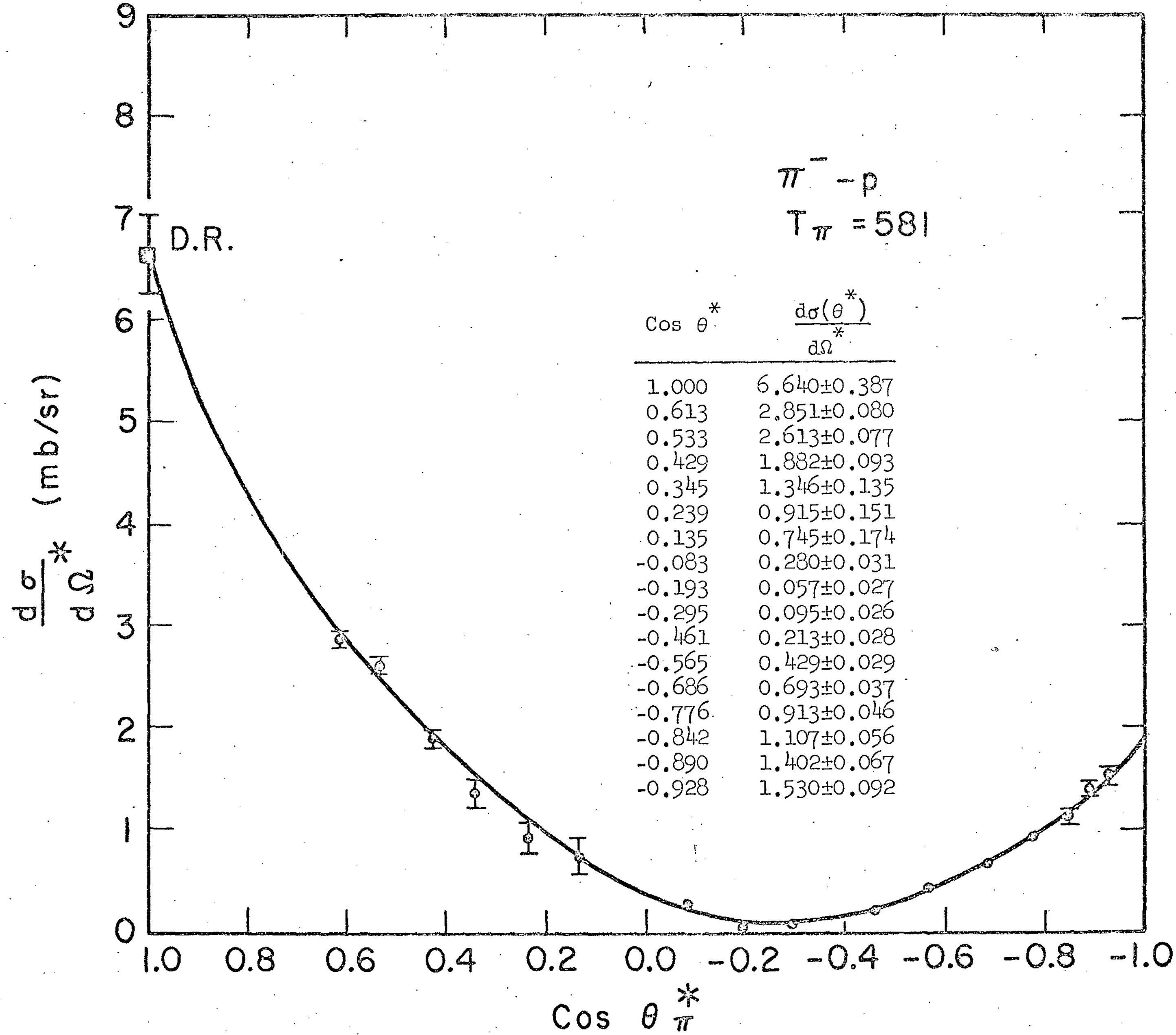

Cos θ^*	$\frac{d\sigma(\theta^*)}{d\Omega^*}$
1.000	6.640±0.387
0.613	2.851±0.080
0.533	2.613±0.077
0.429	1.882±0.093
0.345	1.346±0.135
0.239	0.915±0.151
0.135	0.745±0.174
-0.083	0.280±0.031
-0.193	0.057±0.027
-0.295	0.095±0.026
-0.461	0.213±0.028
-0.565	0.429±0.029
-0.686	0.693±0.037
-0.776	0.913±0.046
-0.842	1.107±0.056
-0.890	1.402±0.067
-0.928	1.530±0.092

Fig. 3.

MU-27307-A

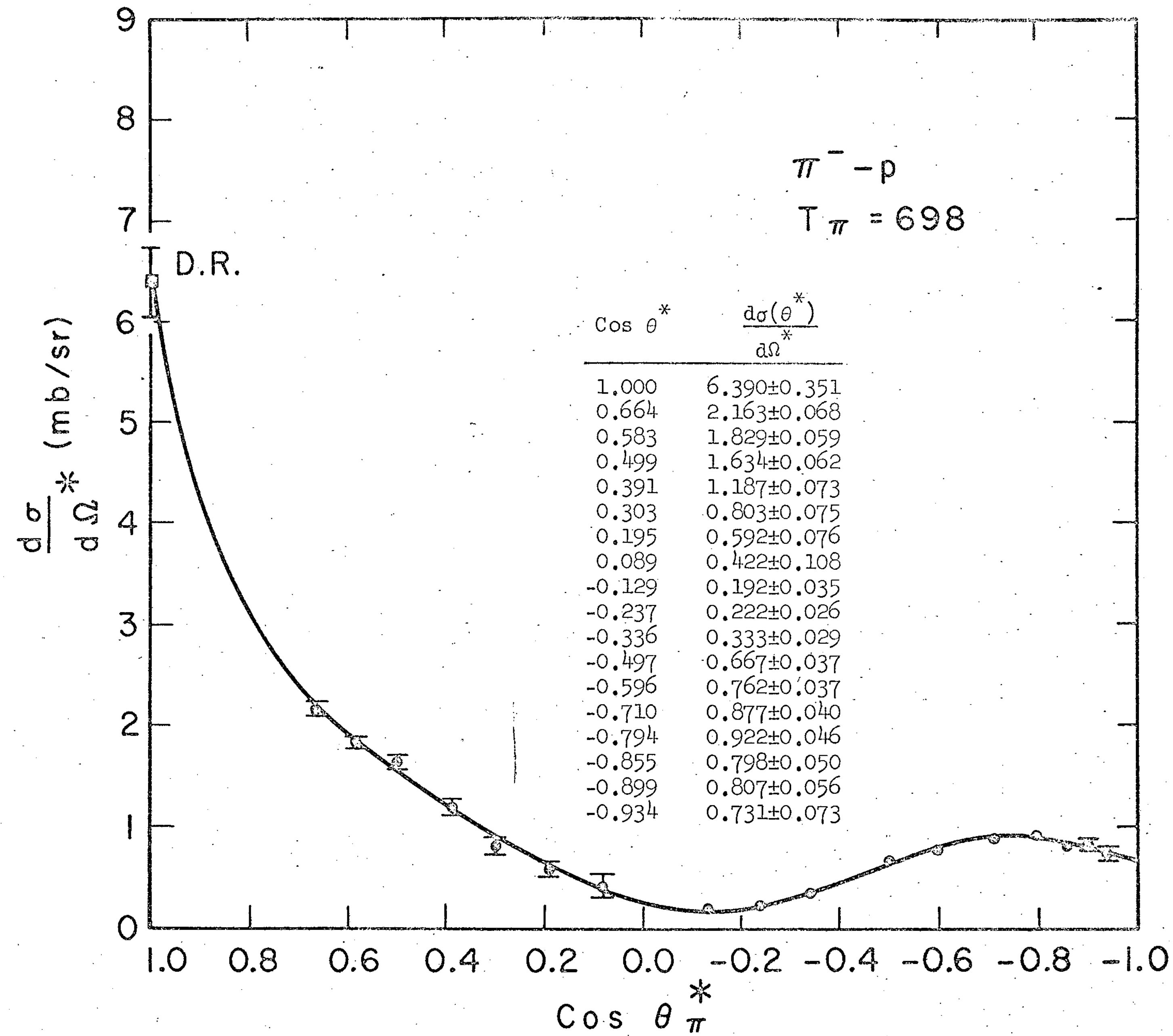

Cos θ^*	$\frac{d\sigma(\theta^*)}{d\Omega^*}$
1.000	6.390±0.351
0.664	2.163±0.068
0.583	1.829±0.059
0.499	1.634±0.062
0.391	1.187±0.073
0.303	0.803±0.075
0.195	0.592±0.076
0.089	0.422±0.108
-0.129	0.192±0.035
-0.237	0.222±0.026
-0.336	0.333±0.029
-0.497	0.667±0.037
-0.596	0.762±0.037
-0.710	0.877±0.040
-0.794	0.922±0.046
-0.855	0.798±0.050
-0.899	0.807±0.056
-0.934	0.731±0.073

Fig. 4.

MU-27306-A

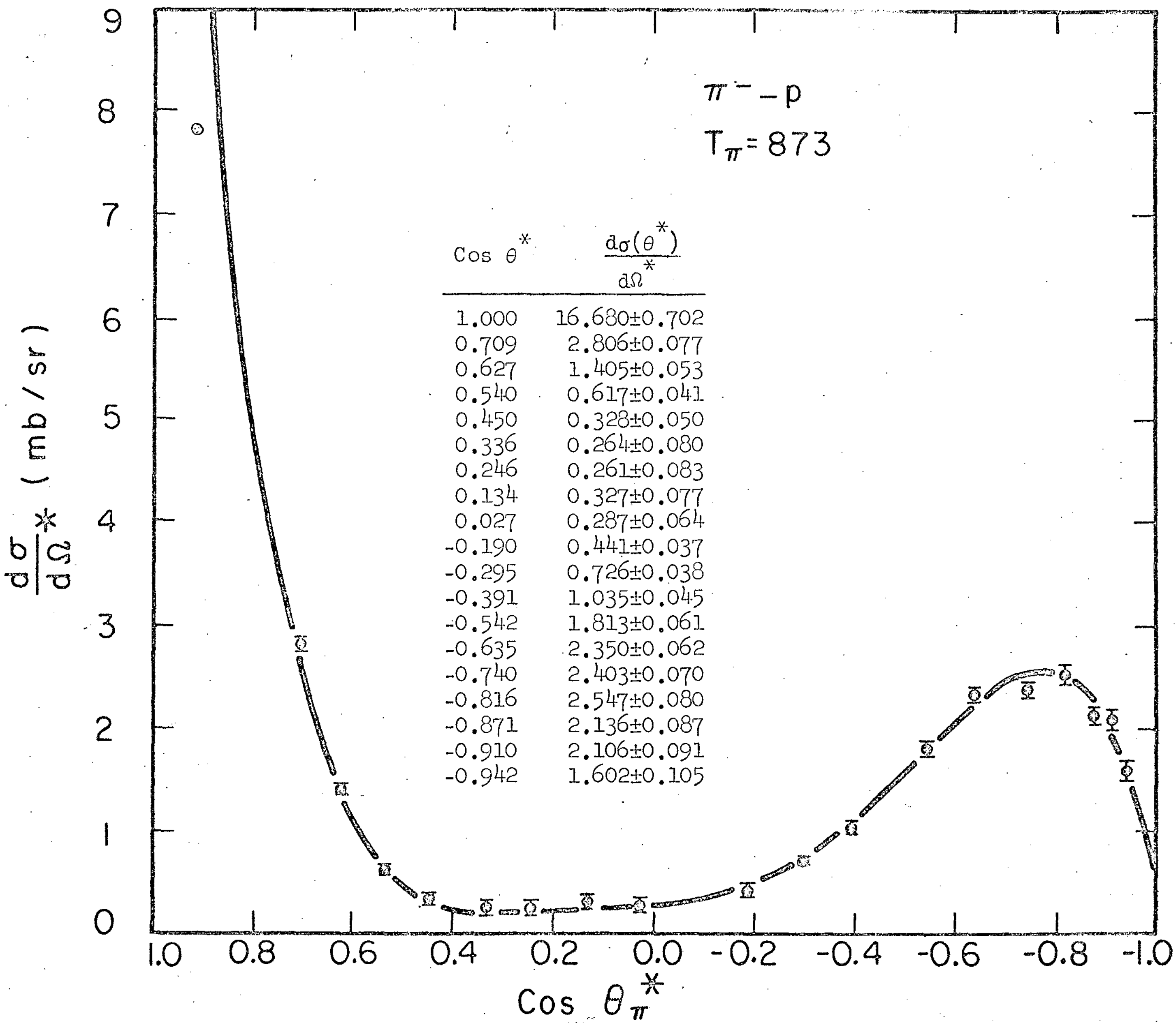

Cos θ^*	$\frac{d\sigma(\theta^*)}{d\Omega^*}$
1.000	16.680±0.702
0.709	2.806±0.077
0.627	1.405±0.053
0.540	0.617±0.041
0.450	0.328±0.050
0.336	0.264±0.080
0.246	0.261±0.083
0.134	0.327±0.077
0.027	0.287±0.064
-0.190	0.441±0.037
-0.295	0.726±0.038
-0.391	1.035±0.045
-0.542	1.813±0.061
-0.635	2.350±0.062
-0.740	2.403±0.070
-0.816	2.547±0.080
-0.871	2.136±0.087
-0.910	2.106±0.091
-0.942	1.602±0.105

Fig. 5.

MU-27305-A

UCRL-10495

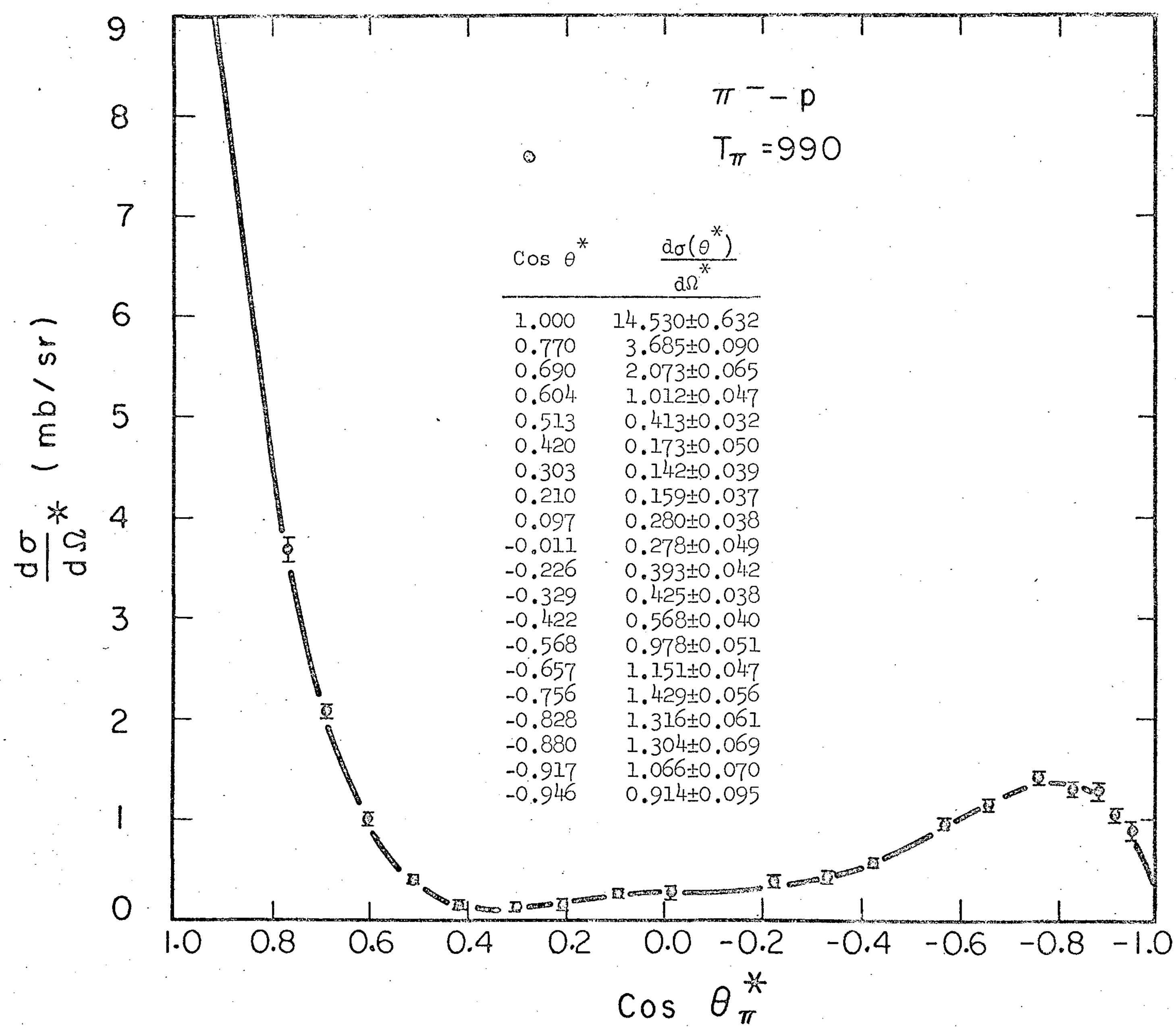

Cos θ^*	$\frac{d\sigma(\theta^*)}{d\Omega^*}$
1.000	14.530±0.632
0.770	3.685±0.090
0.690	2.073±0.065
0.604	1.012±0.047
0.513	0.413±0.032
0.420	0.173±0.050
0.303	0.142±0.039
0.210	0.159±0.037
0.097	0.280±0.038
-0.011	0.278±0.049
-0.226	0.393±0.042
-0.329	0.425±0.038
-0.422	0.568±0.040
-0.568	0.978±0.051
-0.657	1.151±0.047
-0.756	1.429±0.056
-0.828	1.316±0.061
-0.880	1.304±0.069
-0.917	1.066±0.070
-0.946	0.914±0.095

Fig. 6.

MU27304-A

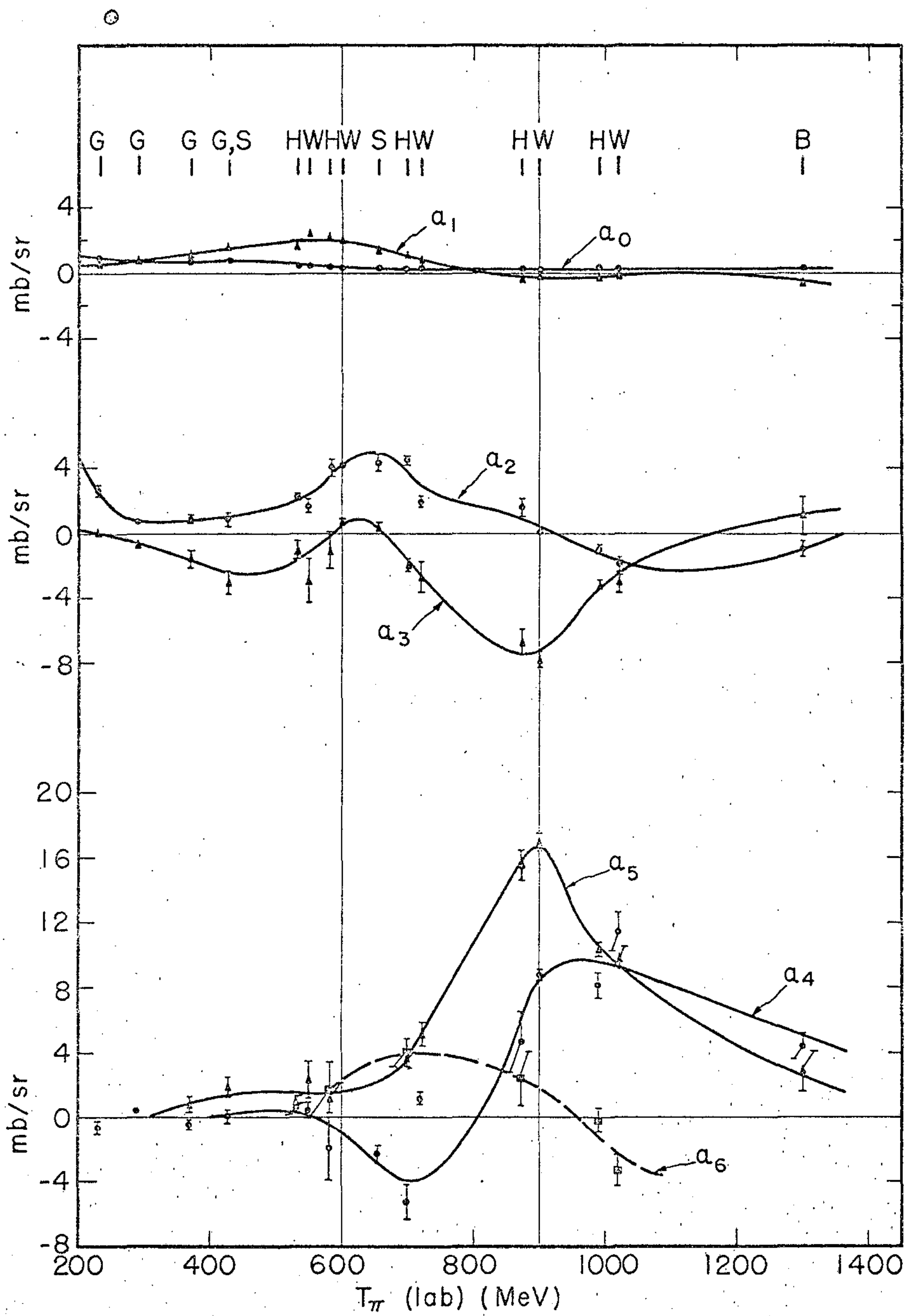

Fig. 7. MUB-1196

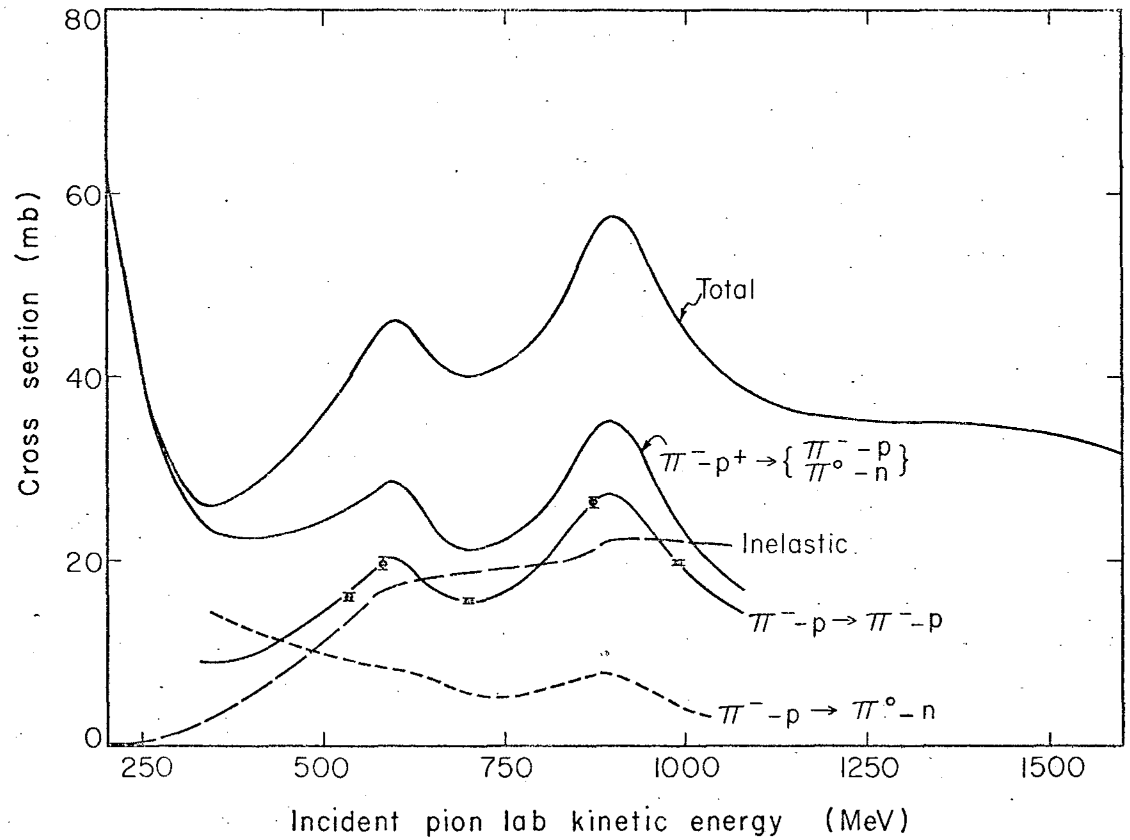

MUB-1354

Fig. 8.

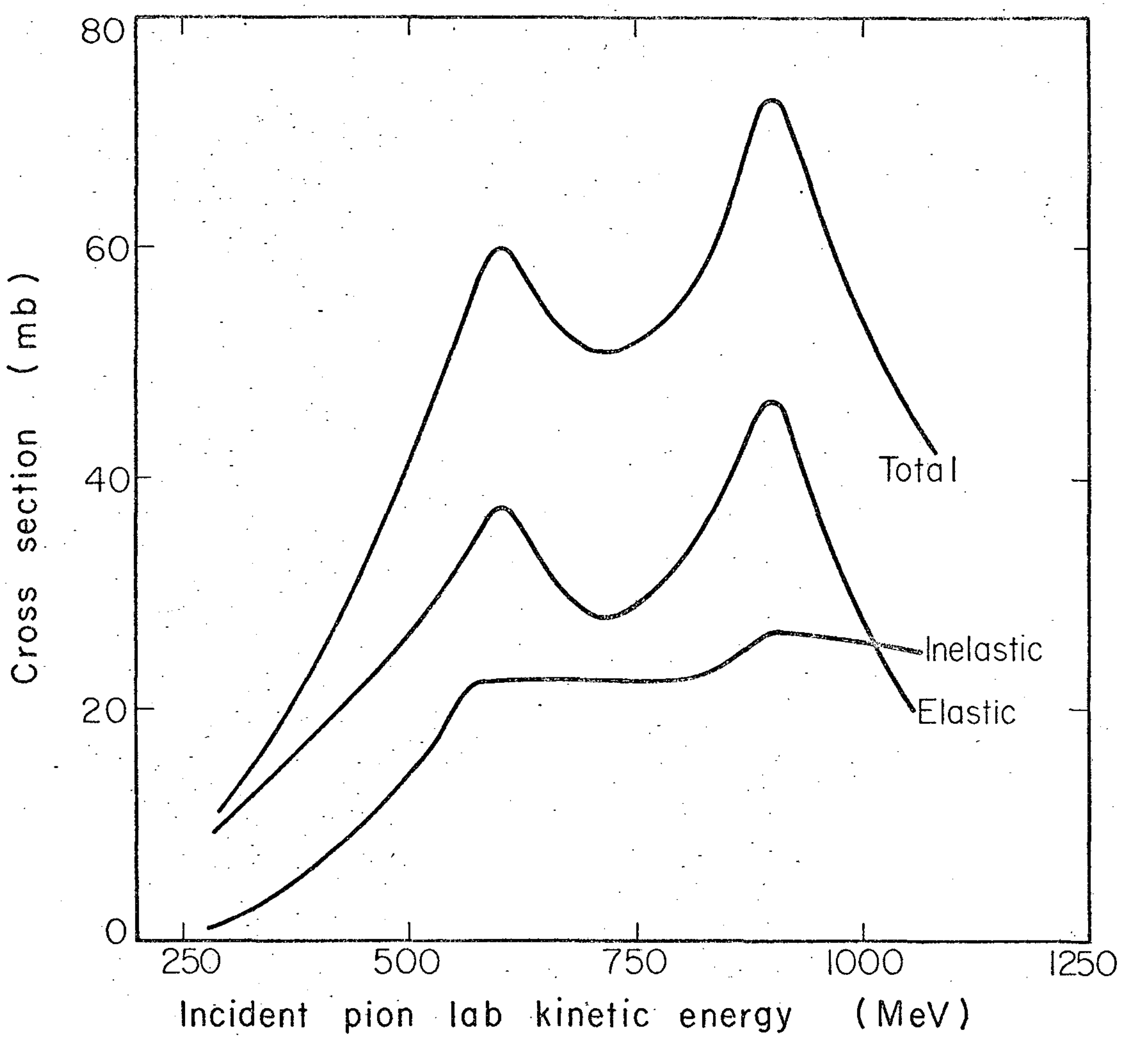

MUB-1355

Fig. 9.

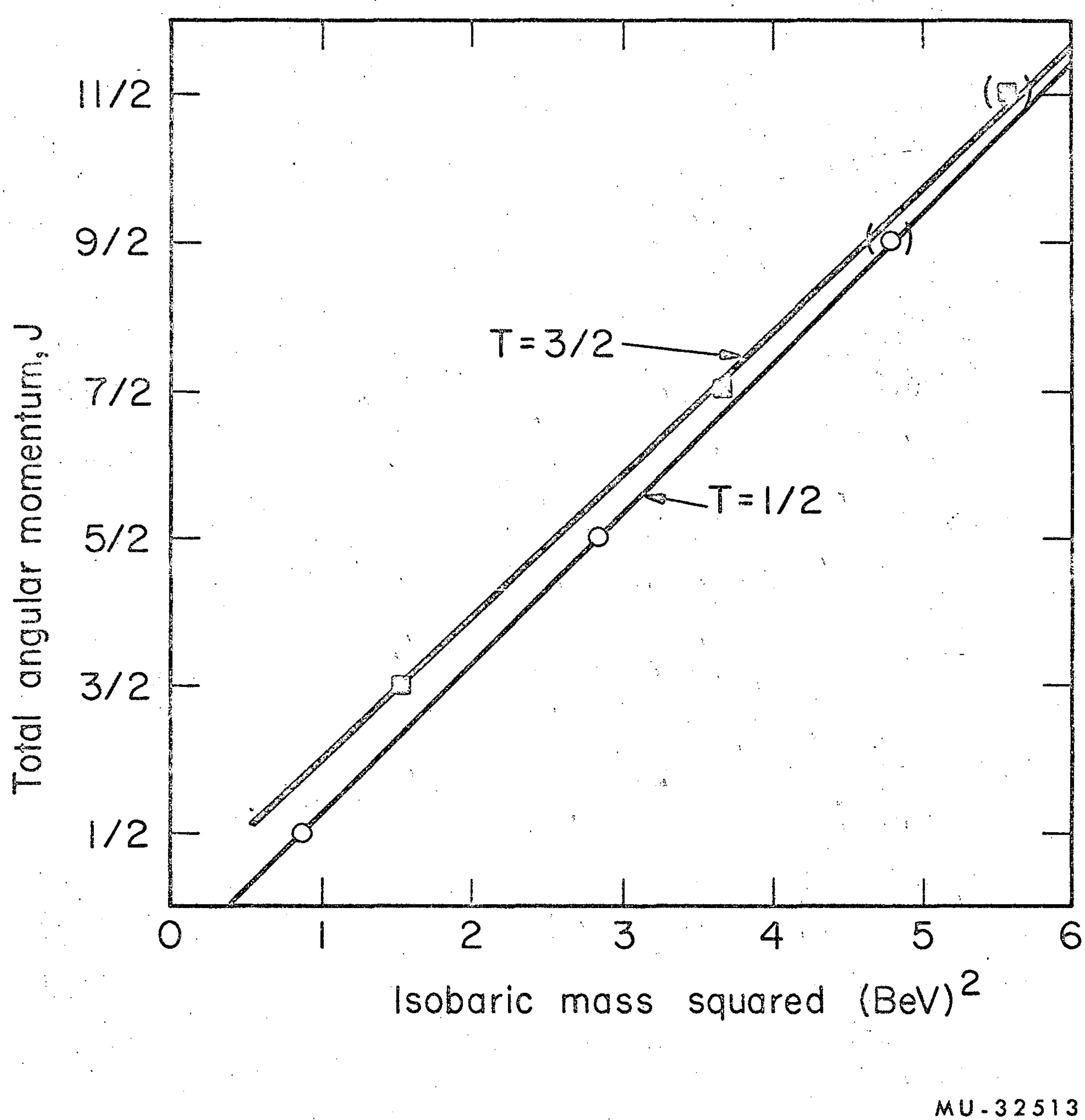
11/2
9/2
7/2
5/2
3/2
1/2
Total angular momentum, J
T=3/2
T=1/2
0
1
2
3
4
5
6
Isobaric mass squared (BeV)2
MU-32513

Fig. 10.